

Finite Element Analysis of 2.5D Woven Composites, Part I: Microstructure and 3D Finite Element Model

Jian Song^{1,2,3} · Weidong Wen^{1,2,3} · Haitao Cui^{1,2,3} ·
Hongjian Zhang^{1,2,3} · Ying Xu^{1,2,3}

Received: 30 April 2015 / Accepted: 6 May 2015 / Published online: 3 June 2015
© Springer Science+Business Media Dordrecht 2015

Abstract A new parameterized finite element model, called the Full-cell model, has been established based on the practical microstructure of 2.5D angle-interlock woven composites. This model considering the surface layer structure can predict the mechanical properties and estimate the structural performance such as the fiber volume fraction and inclination angle. According to introducing a set of periodic boundary condition, a reasonable overall stress field and periodic deformation are obtained. Furthermore, the model investigates the relationships among the woven parameters and elastic moduli, and shows the structural variation along with the corresponding woven parameters. Comparing the results calculated by FEM with the experiments, the veracity of calculation and reasonability based on the Full-cell model are confirmed. In the meantime, the predicted results based on the Full-cell model are more closed to the test results compared to those based on the Inner-cell model.

Keywords 2.5D woven resin composites · Microstructure · Finite element model · Periodic boundary conditions · Geometric characteristics · Mechanical properties

1 Introduction

In recent years, 2.5D woven resin composites have been significant attracted researchers' attention in advanced engineering, owing to their good

✉ Jian Song
dfsongjian2006@126.com

¹ Jiangsu Province Key Laboratory of Aerospace Power System, Nanjing University of Aeronautics and Astronautics, Nanjing, People's Republic of China

² State Key Laboratory of Mechanics and Control of Mechanical Structures, Nanjing University of Aeronautics and Astronautics, Jiangsu 210016, China

³ College of Energy and Power Engineering, Nanjing University of Aeronautics and Astronautics, Nanjing 210016, People's Republic of China

comprehensive mechanics performance. Although the structure is relatively complex in comparison with the laminate composites, 2.5D woven composites provides more advanced properties in the fabric plane and higher delamination resistance than laminates [1, 2]. Therefore, it is of great important to study the microstructure of this class of woven composites so that the mechanical properties are accurately predicted [3].

Until now, some numerical analysis methods have been proposed based on the structure of textile composites. Hallal and Younes [4] proposed an analytical model, called three stages homogenization method, to predict the elastic properties of 2.5D interlock composite. Later, Zheng [5] and Qiu [6] predicted the elastic modulus of 2.5D woven composites based on the selective averaging method. The representative volume element (REV) is first divided into arrays that are decomposed into slices and the iso-stress and iso-strain assumption were used in these slices. Ultimately, the mechanical properties were obtained by the iso-strain assumption once more. Jiang et al. [7] studied the effective modulus of 2D textile composites using a stress and strain averaging procedure. The cell was initially divided into many sub-cells and an averaging was conducted again by assuming uniform stress distribution in each sub-cell to obtain the effective stress and strain of the whole cell. Ishikawa and Chou [8–10] proposed first the bridging model, which was used to analyses the elastic behaviors of 2D woven composites. Tan et al. [11] proposed a new numerical method named as XYZ-model according to a mixed iso-stress and iso-strain to predict the thermo-elastic properties of 3D woven composites. Sankar and Marrey [12] proposed the selective averaging method based on iso-stress assumption to predict the thermo-elastic properties of textile composites.

Finite element method (FEM) has been also used to estimate the mechanical properties of textile composites. Lu et al. [13, 14] studied the failure behaviors of 2.5D textile composites based on the unit cell model and the progressive damage model calculated by FEM were conducted to predict the on-axis and off-axis tensile strength of this class of material. According to the same method, Li and Lu [15, 16] predicted the effective elastic properties of 3D four-directional braided composites based on a new three-dimensional finite element model. Fang [17] established a new damage evolution model according to Murakami-Ohno damage theory to predict the uniaxial tensile behavior of 3D four-directional braided composites. Dong [18] studied the stiffness, strength and damage extended issues of 2.5D woven composites based on commercial finite element analysis software ANSYS.

At present, although several works have analyzed the mechanical properties of 2.5D textile composites by FEM, most of the models only took inner cell into consideration, which inevitable introduces error. Meanwhile, the corresponding mechanical properties of 2.5D woven composites based on finite element analysis are relatively limited and the reasonable periodic boundary conditions for the periodic cell also need to be studied.

In the first part of this work, a realistic parameterized finite element model of 2.5D angle-interlock woven composites considering the outmost layer structure is established. And then the periodic boundary conditions are elaborately given. The validation of the FEM will be further verified by predicting the mechanical properties and the influence of the fiber volume fraction and the inclination angle on the elastic properties of this material are investigated in detail. Additionally, based on the FEM, the geometric characteristics of

the unit cell are analyzed. Finally, comparison validation between experimental data and predicted results is performed.

2 Woven Fabric Structure

In order to improve the simulation precision, it is necessary to investigate the actual microstructure of 2.5D angle-interlock woven composites. Thus, optical photomicrographs of cross sections of composites manufactured by RTM technology were obtained to investigate the configuration of fabric yarns. A typical photomicrograph of 2.5D woven composites (T300/QY8911-IV) was illustrated in Fig. 1. From Fig. 1a, it can be seen that the cross-sectional configurations of weft yarn are diversity and it can be artificially divided into four categories, namely the end weft, the deformed end weft, middle inner weft and middle inner weft. Moreover, the undulations of the warp yarn are significant difference and hence, the warp yarns are defined by two various types: the outer warp and the inner warp, respectively. Figure 1b illustrates that the weft yarn is quasi-straight shape and the cross-sectional configuration of the warp yarn is closed to rectangular shape. Interesting in this structure given in Fig. 1, it is difference from the structures shown in the previous research where the difference between the inner and outer layer was neglected so that the finite model only took the inner cell into account. However, owing to the relatively large differences between the inner and outer layer, it is reasonable to consider the outer structure and establish a more precise finite element model to predict the mechanical properties of 2.5D braided composites. Additionally, since the characteristics of 3D textile structure, the microstructure naturally possesses the smallest repeatable unite (as shown in Fig. 2) which merely considers the inner cell. Therefore, a new model called Full-cell finite element model is proposed based on the following assume:

①A rectangular and two anti-quadratic curve shapes are selected to describe the cross-sections of warp and weft yarns with the interaction in the composites, respectively. ②The weft yarn is assumed to be straight but the outline of the warp yarn is composed of two parts: a quadratic curve in the weft yarn regions depending on the configuration of the weft yarn, and a straight line in the rest part representing the tightening effect in the braiding process. ③The yarn is regarded as unidirectional composite composed of fiber and matrix where the interface between fiber and matrix is ideal.

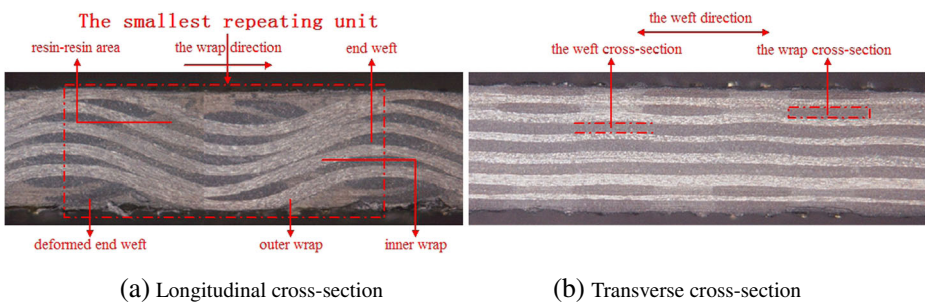


Fig. 1 Cross-sectional photomicrographs of actual 2.5D woven composites (T300/QY8911-IV)

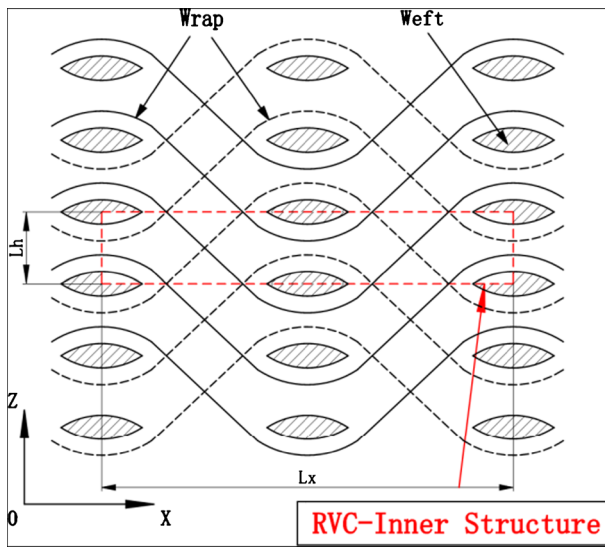


Fig. 2 Microstructure of 2.5D angle-interlock woven composites without the outer layer structure

Additionally, the sizes of the representative unit cell without the outer structure can be obtained from the woven parameters, while the cross-sections of tows can be measured from the microscopic observation. The rest parameters, as illustrated in Figs. 2 and 3 (In these images, the axes x, y, z are defined as longitudinal, transverse and thickness direction), can be calculated as follows:

- The boundary dimensions of the inner cell

$$L_x = 10(N_f - 1)/M_w, L_y = 10N_j/M_j \tag{1}$$

where L_x and L_y are the longitudinal and transverse length (mm), respectively. N_f means the number of weft yarn at the same height in which $N_f=3$. N_j means the number of warp yarn in the transverse direction, in which $N_j=2$. M_j and M_w represent the warp and weft arranged density, in which $M_j=10$ (tows/cm) and $M_w=3.5$ (tows/cm).

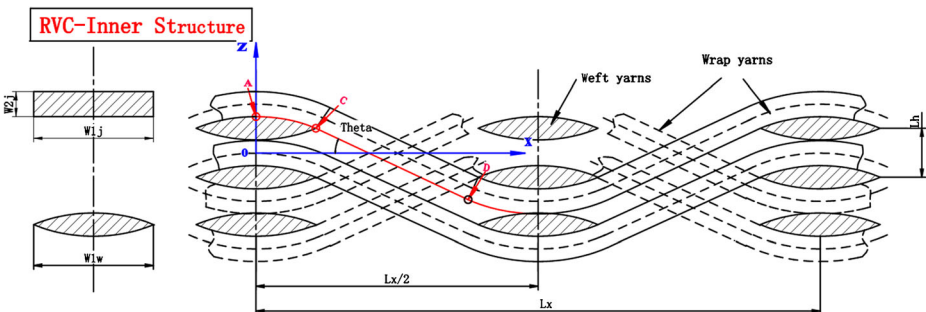


Fig. 3 Illustration of the geometric relation in the inner structure (Local amplification of Fig. 2)

- The cross-sectional sizes of the warp yarn

$$A_j = \frac{T}{1000\rho P_j}, W_{1j} = \frac{10}{M_j}, W_{2j} = \frac{A_j}{W_{1j}} \tag{2}$$

where A_j is the cross-sectional area of warp yarn (mm²). T is the linear density of yarns (g/1000 m). ρ is the material density (g/cm³). P_j is the packing factor of fiber in warp yarn.

- The cross-sectional sizes of the weft yarn and dip angle

$$A_w = \frac{T}{1000\rho P_w}, W_{2w} = \frac{L_z - (N_h + 1)W_{2j}}{N_h - 2} \tag{3}$$

where A_w is the cross-sectional area of weft yarn (mm²). L_z is the height in the z direction.

In order to obtain the width of weft yarn W_{2w} and the dip angle of the straight segment of the warp yarn θ . A series of equations were given in Eqs. 4–8. Furthermore, the configuration of the weft yarn is assumed quadratic curve presented as follows:

$$z = ax^2 + bx + c \tag{4}$$

Firstly, a condition of the first-order continuous in point C (shown in Fig. 3) must be ensure the smooth transition in that point where the two curves are connected.

$$z'|_{x=W_{1w}/2} = -\tan\theta = 2a \cdot \frac{W_{1w}}{2} \tag{5}$$

where θ is the dip angle. In addition, the dip angle can also be described by Eq. 6.

$$\tan\theta = \frac{W_{2j} + W_{2w} + W_{2j}\cos\theta}{L_x/2 - W_{1w} - W_{2j}\sin\theta} \tag{6}$$

By Eq. 6, the dip angle can be obtained by the bisection method on the condition of the known W_{1w} . Furthermore, according to the continuity condition in point A and C, another Eq. 7 can be obtained.

$$c = \frac{W_{2j}}{2} + W_{2w}, \frac{W_{2j} + W_{2w}}{2} = a \left(\frac{W_{1w}}{2}\right)^2 + b \left(\frac{W_{1w}}{2}\right) + c \tag{7}$$

Finally, the configuration of weft yarn is changed by adjusting W_{1w} to make sure that the area of weft yarn is equal to A_w .

$$4 \int_0^{W_{1w}/2} \left(ax^2 + bx + c - \frac{W_{2j} + W_{2w}}{2}\right) dx = A_w \tag{8}$$

Therefore, the shape parameters (W_{1w} , a , c) and dip angle θ can be calculated according to simultaneous Eqs. 4–8. Ultimately, the Inner-cell model shown in Figs. 2 and 3 can be established by the above parameters, as shown in Fig. 4.

The Full-cell model can be then established based on the Inner-cell model which can be obtained by mentioned method. In my view, the reason for formatting this type

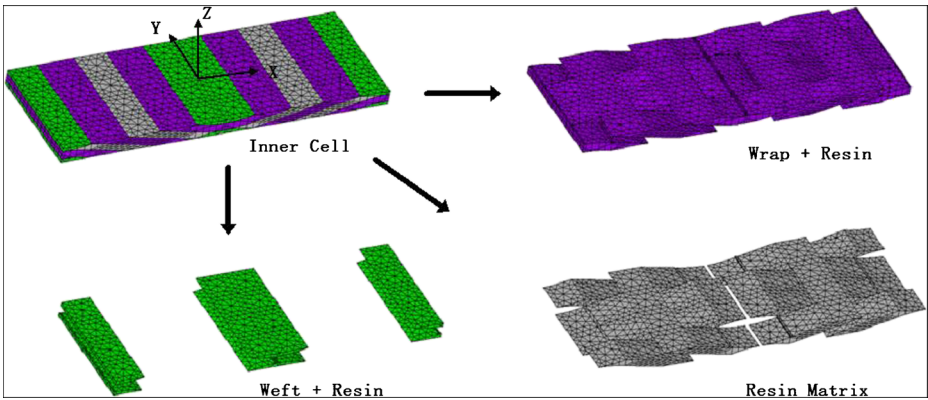


Fig. 4 Microstructure finite element model of 2.5D woven composites without outer cell

of complex microstructure is due to the influence of molding pressure which leads to the fact that the outer weft yarn deviate the center line of the inner weft yarn. Figure 5 illustrates the forming process of 2.5D woven composites based on RTM technology. From Fig. 5, it can be clearly seen that the outer weft yarn is squeezed deviated from the center line and the configuration of that is determined by three aspects: the outermost layer warp yarn (closed to horizontal) and the two secondary layer warp yarns which are upward or downward extension. Similarly, the middle inner or outer weft yarn is generated by four warp yarns: two upward warp yarns and two downward warp yarns. To sum up, based on the assumptions, the sizes calculated by braided parameters and the Inner-cell model, a new model with outer cell can be established in this work as illustrated in Fig. 6.

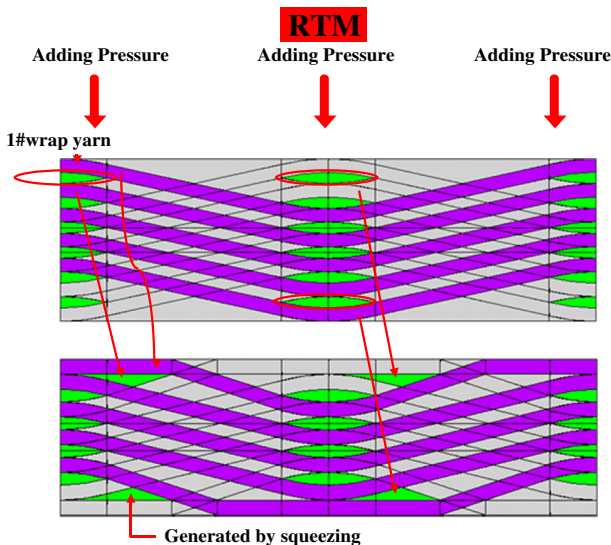


Fig. 5 Molding process of 2.5D woven composites based on RTM technology

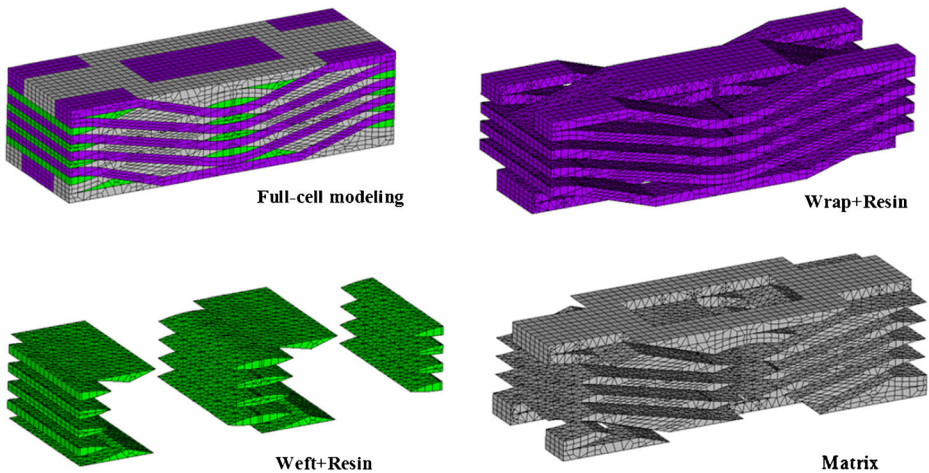


Fig. 6 Full-Cell finite element model of 2.5D angle-interlock woven composites

3 Boundary Conditions of the FEM

Woven composites can be envisaged as a periodical array of the RVEs. In order to assure forces continuity and displacements compatibility of the opposite faces of the representative volume unit cell (RVC) with/ without the outer cell, the periodic boundary conditions (BCs) should be imposed in this simulation. Additionally, the periodic conditions of the inner RVC is more complicated than that of the Full-Cell model owing to taking the extra conditions in Z direction into account. Thus, the periodic boundary conditions for the inner RVC considering six independent macroscopic deformational cases ($\epsilon_x, \epsilon_y, \epsilon_z, \gamma_{xy}, \gamma_{xz}, \gamma_{yz}$) are studied as follows.

Suquet [19] in 1987 stated that for any parallelepiped RVC models, the periodicity can be expressed as Eq. 9 on the boundary ∂V .

$$u_i = \bar{\epsilon}_{ik}x_k + u_i^* \tag{9}$$

where $\bar{\epsilon}_{ik}$ is the average strain. u_i^* is the periodic part of the displacement items on the boundary surfaces but unfortunately, it is generally unknown. Xia [20] in 2003 proposed a more explicit form of periodic boundary conditions based on the above general expression. This is for any parallelepiped RVC models, such as a cubic structure, the following unified periodic boundary conditions are obtained:

$$u_i^{j+}(x, y, z) - u_i^{j-}(x, y, z) = c_i^j \quad (i, j = 1, 2, 3) \tag{10}$$

where c_1^1, c_2^2 and c_3^3 correspond to the normal deformations, whereas the other three pairs of constants, $c_1^2(c_2^1), c_1^3(c_3^1)$ and $c_2^3(c_3^2)$ correspond to the shear deformations.

To describe Eq. 10 in the FEM software using, the periodic boundary conditions are achieved by using the discrete nodes which exist in the opposite surfaces, edges and vertices of the cubic RVC model. All of the constraint equations applied in the FEM software will be given as followed in accordance with the cubic structure as shown in Fig. 7.

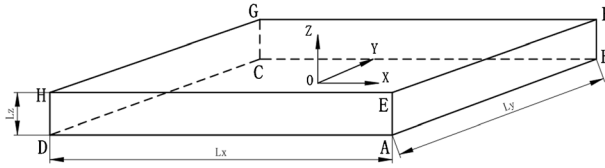


Fig. 7 Cuboid-shaped unit and its geometric dimensions

- For three groups of the opposite surfaces:
 - I. the opposite surfaces perpendicular to X, Y and Z axis:

$$\begin{cases} u|_{x=L_x/2} - u|_{x=-L_x/2} = L_x \varepsilon_x \\ v|_{x=L_x/2} - v|_{x=-L_x/2} = 0 \\ w|_{x=L_x/2} - w|_{x=-L_x/2} = 0 \end{cases} \tag{11}$$

$$\begin{cases} u|_{y=L_y/2} - u|_{y=-L_y/2} = L_y \gamma_{xy} \\ v|_{y=L_y/2} - v|_{y=-L_y/2} = W_y \varepsilon_y \\ w|_{y=L_y/2} - w|_{y=-L_y/2} = 0 \end{cases} \tag{12}$$

$$\begin{cases} u|_{z=L_z/2} - u|_{z=-L_z/2} = L_z \gamma_{xz} \\ v|_{z=L_z/2} - v|_{z=-L_z/2} = L_z \gamma_{yz} \\ w|_{z=L_z/2} - w|_{z=-L_z/2} = L_z \varepsilon_z \end{cases} \tag{13}$$

- For 12 edges divided into three types:
 - ①AD, BC, FG and EH parallel to X axis.
 - ②CD, BA, EF and HG parallel to Y axis.
 - ③HD, EA, FB and GC parallel to Z axis.
 - I. the edges parallel to X axis

$$\begin{cases} u|_{BC} - u|_{AD} = L_y \gamma_{xy} \\ v|_{BC} - v|_{AD} = L_y \varepsilon_y \\ w|_{BC} - w|_{AD} = 0 \end{cases} \tag{14}$$

$$\begin{cases} u|_{FG} - u|_{AD} = L_y \gamma_{xy} + L_z \gamma_{xz} \\ v|_{FG} - v|_{AD} = L_y \varepsilon_y + L_z \gamma_{yz} \\ w|_{FG} - w|_{AD} = L_z \varepsilon_z \end{cases} \tag{15}$$

$$\begin{cases} u|_{EH} - u|_{AD} = L_z \gamma_{xz} \\ v|_{EH} - v|_{AD} = L_z \gamma_{yz} \\ w|_{EH} - w|_{AD} = L_z \varepsilon_z \end{cases} \tag{16}$$

For the other edges, the corresponding periodic boundary conditions can be obtained refer to Eqs. 14~15.

- For eight vertices: the constraint equations are established between the vertex D and the rest of vertices.
 - I. the vertices of E, F, G and D

$$\begin{cases} u|_E - u|_D = L_x \varepsilon_x + L_z \gamma_{xz} \\ v|_E - v|_D = L_z \gamma_{yz} \\ w|_E - w|_D = L_z \varepsilon_z \end{cases} \tag{17}$$

$$\begin{cases} u|_F - u|_D = L_x \varepsilon_x + L_y \gamma_{xy} + L_z \gamma_{xz} \\ v|_F - v|_D = L_y \varepsilon_y + L_z \gamma_{yz} \\ w|_F - w|_D = L_z \varepsilon_z \end{cases} \tag{18}$$

$$\begin{cases} u|_G - u|_D = L_y \gamma_{xy} + L_z \gamma_{xz} \\ v|_G - v|_D = L_y \varepsilon_y + L_z \gamma_{yz} \\ w|_G - w|_D = L_z \varepsilon_z \end{cases} \tag{19}$$

For the other vertices, the corresponding periodic boundary conditions can be obtained refer to Eq.

According to the discrete method mentioned above, it is convenient to adopt Eq. 11~29 in a finite element procedure, instead of applying Eq. 10 directly as the boundary conditions. In addition, It is assumed that the average mechanical properties of a RVC are equal to the average properties of 2.5D woven composites. The average stresses σ_{ij} in the case of given strains ε_{ij} are defined by

$$\bar{\sigma}_{ij} = \frac{1}{V} \int_V \sigma_{ij} dV \tag{20}$$

By using the Gauss integral and equilibrium equation $\sigma_{ij,j}=0$, the average stress can be expressed as

$$\bar{\sigma}_{ij} = \frac{1}{V} \int_S \sigma_{ik} x_{j,n} n_k dS \tag{21}$$

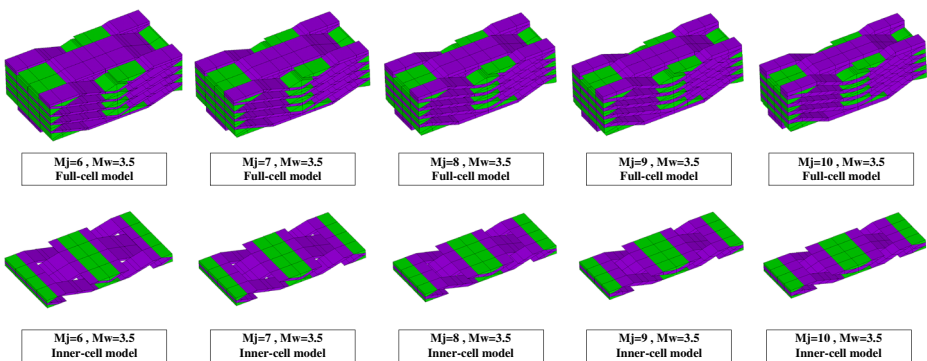


Fig. 8 3D finite element model of 2.5D woven composites with the M_j increases (Rich-rein regions removed)

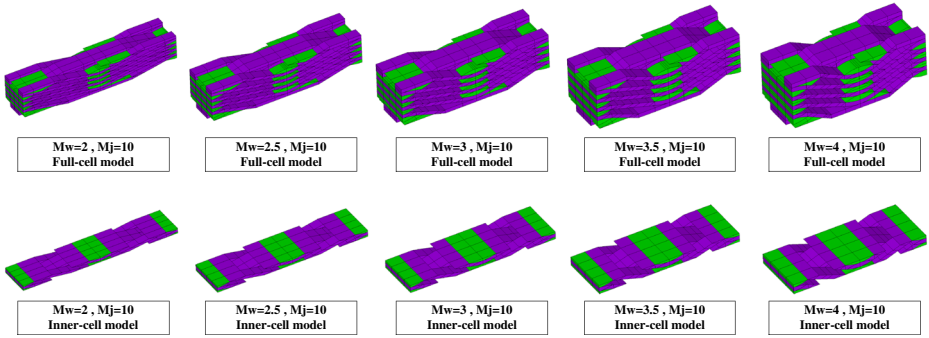


Fig. 9 3D finite element model of 2.5D woven composites with the M_w increases (Rich-rein regions removed)

To satisfy the periodic condition at the opposite boundaries, the related points on the two opposite planes must have the same stresses. Thus, Eq. 31 can be reduced to

$$\bar{\sigma}_{ij} = \frac{1}{V} \left(\int_{S_m^+} \sigma_{im}^+ x_j^+ dS - \int_{S_m^-} \sigma_{im}^- x_j^- dS \right) = \frac{1}{V} \int_{S_m^+} \sigma_{im}^+ (x_j^+ - x_j^-) dS \quad (22)$$

where m is a dummy suffix, when $m \neq j$, the coordinates $x_j^+ = x_j^-$ and when $m = j$, $x_j^+ - x_j^- = \Delta x_j$, therefore,

$$\bar{\sigma}_{ij} = \frac{\Delta x_j}{V} \int_{S_j} \sigma_{ij} dS = \frac{P_{ij}}{S_j}, \text{ (no summation over } j) \quad (23)$$

From Eq. 33, the average stresses can be simply calculated by the resultant tractions on the boundary surfaces and the corresponding boundary surfaces.

In particularly, for the Full-cell model, since the upper and lower boundary is the actual boundary of the 2.5D woven composites, the periodic boundary condition mentioned above

Table 1 Compared results of fiber volume fraction of 2.5D woven composites

	Composite panel I		Composite panel II	
	Woven fabric m_1	Composites m_2	Woven fabric m_1	Composites m_2
Mass (Kg)	422.90	826.50	424.00	820.00
Volume fraction ^a	42.67 %		43.20 %	
Average value	42.94 %			
Predictive value	43.89 %			
Error	2.22 %			

Predictive value is obtained based on the example shown in Section 4.4

^a Fiber volume fraction (measured) $V_f = m_1 / \rho_f (m_1 / \rho_f + (m_2 - m_1) / \rho_m)$, m_1 : pre-casting mass, kg. m_2 : post-casting mass, kg. ρ_f, ρ_m : density of fiber and matrix, respectively. The specific values above parameters are also shown in Section 4.4

Table 2 Compared results of inclination angles of 2.5D woven composites

	Measure values ^a (°)				Average Value (°)	Dispersion Coefficient	Predictive value (°)	Error (%)
	No. 1	No. 2	No. 3	No. 4				
θ_o	18.125	17.216	17.961	17.650	17.738	2.254 %	17.467	1.528
θ_i	21.266	19.797	18.252	21.485	20.200	7.423 %	21.776	7.802

Predictive value is obtained based on the example shown in Section 4.4

^a Measure data are obtained according to observing the microstructure by optical microscopy (HIROX made in Japan)

can be simplified as the boundary condition neglecting the equations corresponding to the Z direction.

4 Results and Discussion

4.1 3D Finite Element Model and Model Verification

Figure 8 illustrates the Full-cell and Inner-cell finite element models with different woven parameters.

According to the Figs. 8 and 9, as the increase of M_j , the width of models decreases steadily under fixed M_w . When M_j is constant, the width of models has an upward trend with the M_w rises.

In order to verify the veracity of this model (Full-cell model), some experiments related to the fiber volume fraction and inclination angle were conducted.

For the Full-cell model, the fiber volume fraction can be calculated as follows:

$$V_f = \frac{n_j P_j V_{j0} + n_w P_w V_{w0}}{L_x L_y L_z} \times 100\% \tag{24}$$

where V_j , V_w and V_f represent the fiber volume fraction of warp, weft and total in a 2.5D woven composites. V_{j0} and V_{w0} are the each component volume fraction directly obtained by finite element software.

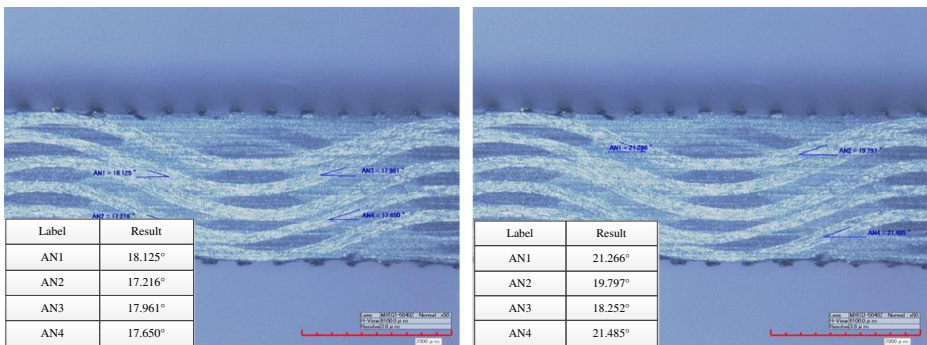


Fig. 10 Measure photographs of inclination angles

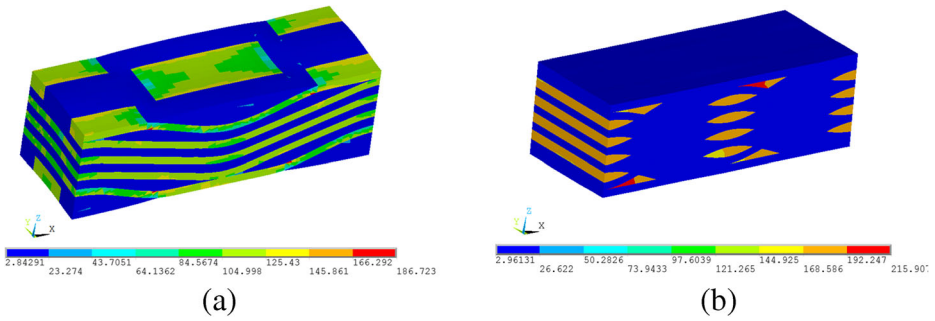


Fig. 11 Deformed von Mises stress nephograms of FEM (a) Deformation under X tensile loading, (b) Deformation under Y tensile loading

Table 1 gives the compared result between the prediction values calculated by Eq. (24) and measured values by weighing method. It can be seen that the error between the experimental measure value and predicted value of fiber volume fracture is only 2.22 %. Additionally, the internal and the outmost layer inclination angles predicted based on Eqs. (1)–(8) and deviation with the test measured results are listed in Table 2 (Fig. 10 shows the corresponding observing results). According to the results, the maximum error is also only 7.802 %. Therefore, the modeling approach proposed in this study is available to establish the finite element model of 2.5D woven composites, precisely.

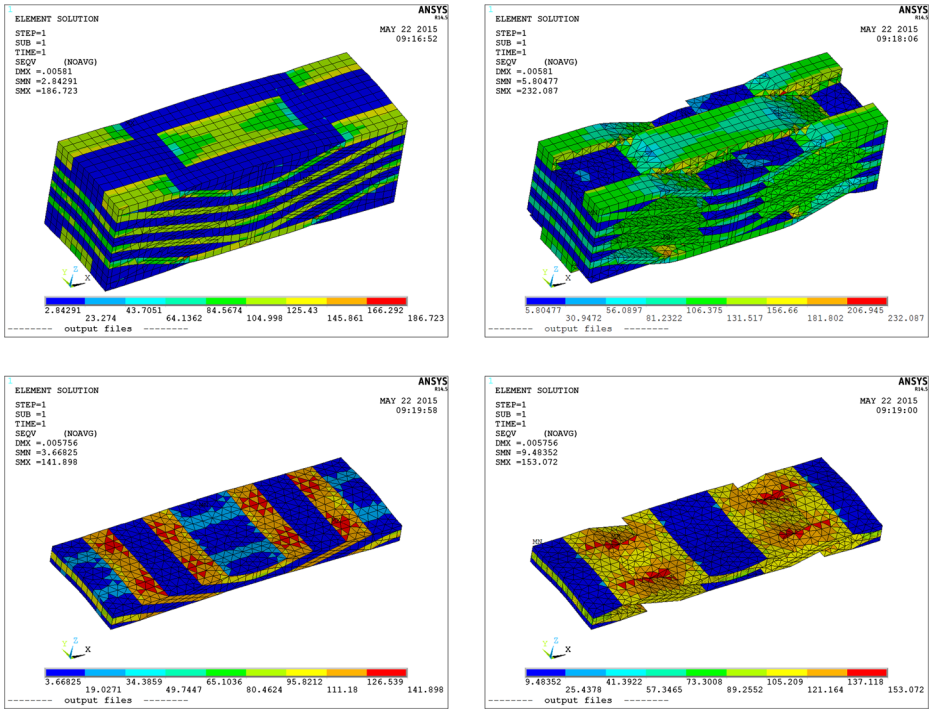


Fig. 12 Stress nephograms of the FEM under tensile loading in the warp direction

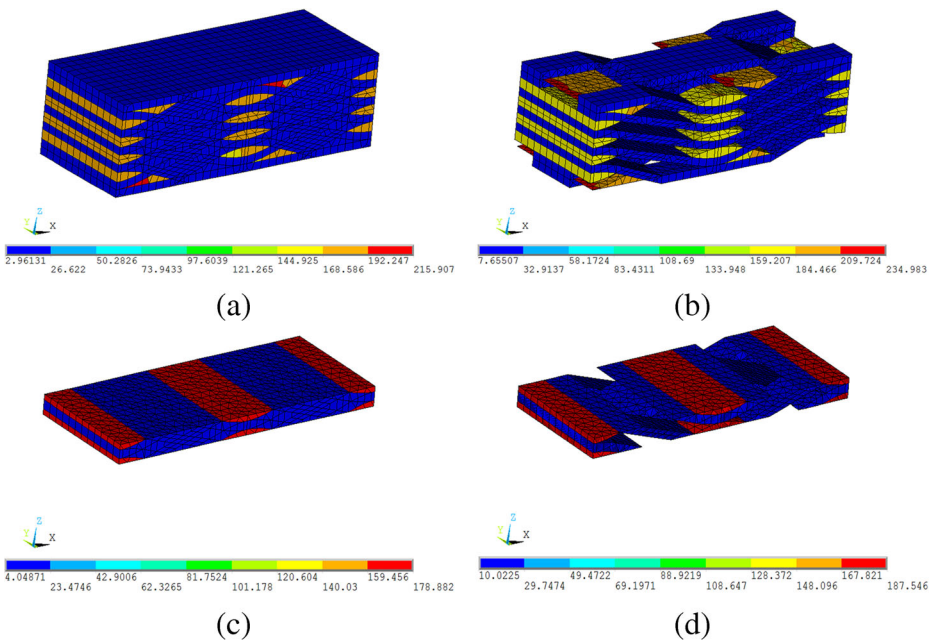


Fig. 13 Stress nephograms of the FEM under tensile loading in the weft direction

4.2 Stress Nephograms of the FEM with/Without the Outmost Layer Structure

Figure 11 shows the stress distribution together with the deformation based on the Full-cell model. According to the Fig. 11, it can be seen that even though the boundary surfaces do not remain plane any more, the opposite surfaces maintain the identical deformation, which suggests that the periodic boundary condition is reasonable. The stress distribution in each yarn shows different stress state but presents a periodic distribution characteristic in X-Y plane (see the Fig. 11a, b). The main reason for these phenomena is that the requirement of the

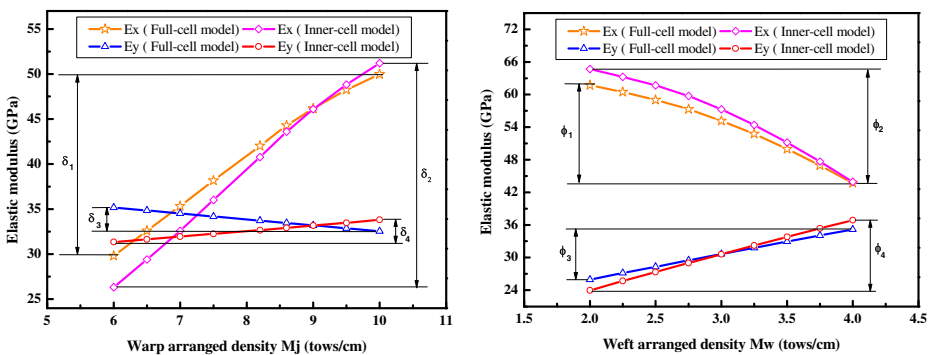


Fig. 14 Effect of (a) M_j and (b) M_w on the effective elastic constants. δ_i ($i=1,2$) and φ_i ($i=1,2$) represent the maximum variation of E_x and E_y based on different models, respectively. For the performance of E_x , $\delta_1=+20.17\text{GPa}$, $\delta_2=+24.87\text{GPa}$, $\delta_3=-2.62\text{GPa}$, $\delta_4=+2.47\text{GPa}$. For the performance of E_y , $\varphi_1=-17.99\text{GPa}$, $\varphi_2=-20.76\text{GPa}$, $\varphi_3=+9.21\text{GPa}$, $\varphi_4=+12.91\text{GPa}$

Table 3 Material parameters of the specimens

	E_{j1}/E_m	E_{j2}	G_{j12}/G_m	G_{j23}	u_{j12}/u_m
T300-3 K	230	40	17	4.8	0.3
QY8911-IV	4.16	–	–	–	0.34

periodical condition mentioned above and the spatial geometrical structure complexity of the yarns in 2.5D woven composites.

Figure 12 presents the stress nephogram of the component materials under tensile loading in the warp direction (X direction as well). As can be seen from the Fig. 12a and b, the stress levels in warp yarns are obviously greater than that in weft yarns, aiming at about 40 times, which indicates that the warp yarns are the primary load-carrying objects when the load is paralleled to the warp direction. Additionally, from Fig. 12c and d, an obvious stress concentration can be found in the crossing points of warp yarns, and the stress states of internal inclination warp yarns are more seriously than other parts of the corresponding warp yarns (see Fig. 12d), suggesting that the damages, such as transverse micro-cracks, might be preliminary generated in these regions subjected to the load in the warp direction. The stress concentration phenomenon is produced in the contact edges of warp yarns caused by the tensile and shear stress.

Figure 13 presents the stress nephogram of the component materials under the load in the weft direction. The maximum value of stress in the weft yarns is approximately 30 times more than that in the warp yarns, indicating that the weft yarns are main load-carrying objects (see Fig. 13a). Furthermore, the stress concentrations are observed at the outmost lay weft yarns (see Fig. 13b), which indicates that the initial damage might be found in these domains. Although the stress concentration phenomenon still exists, uniform stress field has been found in the internal weft yarns, which almost bear entire load in the weft direction (Fig. 13c and d).

4.3 Discussion on the Elastic Modulus Properties

Figure 13 illustrates the variation of the elastic moduli E_x and E_y with the main woven parameters M_j and M_w .

In general, it can be found from the Fig. 14 that the variation trends and related values of E_x and E_y calculated based on the Full-cell model are consistent with those based on the Inner-cell model. Although an opposite change tendency consists in the performance of E_y with the M_j increases, the variation values are quite small ($\delta_3 = -2.62\text{GPa}$, $\delta_4 = +2.47\text{GPa}$). Thus, it can be recognized that the influence of M_j on the E_y is basically unchangeable.

Table 4 Woven parameters of the specimens

	$M_w(\text{tows/cm})$	$M_w(\text{tows/cm})$	N_f	N_h	$L_z(\text{mm})$
S1 ^{a*}	10	3.5	3	6	1.95
S2 ^{b*}	10	3.5	3	6	1.95

a* (b*) represent that the specimens subjected to the uniaxial load in the warp (weft) direction

Table 5 Prediction results in comparison with test data

	Experimental average (range)	Prediction			
		Full-cell model	Error	Inner-cell model	Error
E_x (GPa)	48.39 (46.71–50.24)	49.96	3.24 %	51.20	5.81 %
E_y (GPa)	32.30 (29.67–34.79)	32.55	0.77 %	33.81	4.67 %

4.4 Compared with the Experimental Results

In order to verify the validity of the FEM, a total of 10 specimens (T300-3 K/QY8911-IV) made by RTM technics were prepared along the warp (6 specimens) and weft (4 specimens) directions, respectively. An MTS 810 hydraulic servo dynamic material test machine with a 25.4 mm MTS-634-25 extensometer was used to perform the tests at room temperature (20 °C). The material parameters and woven parameters of specimens are shown in Tables 3 and 4. The corresponding results are illustrated in Table 3.

Good coincidence between experimental and theoretical prediction based on the Full-cell model results suggests the feasibility of the proposed model and method in predicting the elastic properties of 2.5D angle-interlock woven resin matrix composites. Additionally, the prediction results based on the Full-cell model are more close to the related test results than those based on the Inner-cell model, especially the weft modulus (Table 5).

5 Conclusion

In this work, a new parameter FEM based on the microstructure of 2.5D angle-interlock woven resin composites has been established and some meaning conclusions are presented as follows:

- (1) The face structure has been taken into consideration in this work, and the more precise prediction results of fiber volume fraction and inclination angle based on the model can be obtained compared to those only considering the internal model.
- (2) A comparison of finite element predicting based on Full-model and experimental results demonstrate the validity of the proposed model in predicting the elastic properties of 2.5D woven composites.
- (3) According to analyzing the stress nephogram, the periodic stress distribution indicates that the periodic boundary condition proposed in this work is reasonable, which can guarantee the continuity of the displacement. Furthermore, the reasonable overall stress fields exhibit that the stress concentration phenomenon is more serious in the surface layer than that in the interior.
- (4) Based on the Full-cell model, the modulus E_x is increased obviously with the increase of the warp arrange density M_j , however, it decreases significantly as the weft arrange density M_w increases. According to the Inner-cell model, the influence of M_j on the E_x is slight, with only $-2.62\text{GPa}\sim+2.47\text{GPa}$ affected.
- (5) The main effective elastic moduli are obtained based on the Full-cell model and Inner-cell model using the finite analysis approach. The results show that the theoretical results are suitable for the experimental results and the theoretical method is validity.

Further work will focus on the mechanical behavior analysis, strength predictive method and damage mechanism research of 2.5D woven composites under the tensile loading in the warp (or the weft) direction.

Acknowledgments The work was supported by Jiangsu Innovation Program for Graduate Education [grant number KYLX_0237].

Compliance with Ethical Standards All authors have read and approved this version of the article, and due care has been taken to ensure the integrity of the work. Neither the entire paper nor any part of its content has been published or has been accepted elsewhere. It is not being submitted to any other journal. We wish the paper may be of particular interest to the readers of your journal.

References

- Mouritz, A.P., Bannister, M.K., Falzon, P.J., et al.: Review of applications for advanced three-dimensional fibre textile composites[J]. *Compos. A: Appl. Sci. Manuf.* **30**(12), 1445–1461 (1999)
- Sarikanat, M., Sever, K., Seki, Y., et al.: Mechanical anisotropy in unidirectional glass fabric reinforced oligomeric siloxane modified polyester composites[J]. *Fibers Polym.* **13**(6), 775–781 (2012)
- Ayranci, C., Carey, J.: 2D braided composites: a review for stiffness critical applications[J]. *Compos. Struct.* **85**(1), 43–58 (2008)
- Hallal, A., Younes, R., Fardoun, F., et al.: Improved analytical model to predict the effective elastic properties of 2.5 D interlock woven fabrics composite[J]. *Compos. Struct.* **94**(10), 3009–3028 (2012)
- Zheng, J.: Research on elastic property prediction and failure criteria of 2.5D woven composites[D]. Nanjing University of Aeronautics and Astronautics. (2008)
- Qiu, R.: Research on fatigue life prediction and damage analysis of 2.5D woven composites[D]. Nanjing University of Aeronautics and Astronautics. (2014)
- Jiang, Y., Tabiei, A., Simitses, G.J.: A novel micromechanics-based approach to the derivation of constitutive equations for local/global analysis of a plain-weave fabric composite[J]. *Compos. Sci. Technol.* **60**(9), 1825–1833 (2000)
- Ishikawa, T., Chou, T.: Elastic behavior of woven hybrid composites[J]. *J. Compos. Mater.* **16**(1), 2–19 (1982)
- Ishikawa, T., Chou, T.: Stiffness and strength behaviour of woven fabric composites[J]. *J. Mater. Sci.* **17**(11), 3211–3220 (1982)
- Chou, T., Ishikawa, T.: One-dimensional micromechanical analysis of woven fabric composites[J]. *AIAA J.* **21**(12), 1714–1721 (1983)
- Tan, P., Tong, L., Steven, G.P.: Micromechanics models for mechanical and thermomechanical properties of 3D through-the-thickness angle interlock woven composites[J]. *Compos. A: Appl. Sci. Manuf.* **30**(5), 637–648 (1999)
- Sankar, B.V., Marrey, R.V.: Analytical method for micromechanics of textile composites[J]. *Compos. Sci. Technol.* **57**(6), 703–713 (1997)
- Lu, Z., Zhou, Y., Yang, Z., et al.: Multi-scale finite element analysis of 2.5 D woven fabric composites under on-axis and off-axis tension[J]. *Comput. Mater. Sci.* **79**, 485–494 (2013)
- Zhou, Y., Lu, Z., Yang, Z.: Progressive damage analysis and strength prediction of 2D plain weave composites[J]. *Compos. Part B* **47**, 220–229 (2013)
- Li, D., Fang, D., Lu, Z., et al.: Finite element analysis of mechanical properties of 3D four-directional rectangular braided composites—Part 2: validation of the 3D finite element model[J]. *Appl. Compos. Mater.* **17**(4), 389–404 (2010)
- Li, D., Lu, Z., Lu, W.: Theoretical prediction of stiffness and strength of three-dimensional and four-directional braided composites[J]. *Appl. Math. Mech.* **29**, 163–170 (2008)
- Guo-Dong, F., Jun, L., Bao-Lai, W.: Progressive damage and nonlinear analysis of 3D four-directional braided composites under unidirectional tension[J]. *Compos. Struct.* **89**(1), 126–133 (2009)
- Dong, W.F., Xiao, J., Li, Y.: Finite element analysis of the tensile properties of 2.5 D braided composites[J]. *Mater. Sci. Eng. A* **457**(1), 199–204 (2007)
- Suqut, P.: Elements of homogenization theory for inelastic solid mechanics. In: Sanchez-Palencia, E., Zaoui, A. (eds.) *Homogenization techniques for composite media*. Berlin: Springer-Verlag (1987)
- Xia, Z.H., Zhou, C.W., Yong, Q.L., and Wang, X.W.: On selection of repeated unit cell model and application of unified periodic boundary conditions in micromechanical analysis of composites. *Int. J. Solids. Struct.* **43**(2), 266–278 (2006)